

Coupled bulk and brane fields about a de Sitter brane

Antonio Cardoso,^{*} Kazuya Koyama,[†] Andrew Mennim,[‡] Sanjeev S. Seahra,[§] and David Wands[¶]
Institute of Cosmology & Gravitation, University of Portsmouth, Portsmouth PO1 2EG, UK

(Dated: December 19, 2006)

We consider the evolution of a bulk scalar field in anti-de Sitter (AdS) spacetime linearly coupled to a scalar field on a de Sitter boundary brane. We present results of a spectral analysis of the system, and find that the model can exhibit both bound and continuum resonant modes. We find that zero, one, or two bound states may exist, depending upon the masses of the brane and bulk fields relative to the Hubble length and the AdS curvature scale and the coupling strength. In all cases, we find a critical coupling above which there exists a tachyonic bound state. We show how the 5-dimensional spectral results can be interpreted in terms of a 4-dimensional effective theory for the bound states. We find excellent agreement between our analytic results and the results of a new numerical code developed to model the evolution of bulk fields coupled to degrees of freedom on a moving brane. This code can be used to model the behaviour of braneworld cosmological perturbations in scenarios for which no analytic results are known.

I. INTRODUCTION

Branes offer an alternative to the traditional Kaluza-Klein approach to dimensional reduction. Some degrees of freedom are restricted to branes, while other fields, including gravity, propagate in the higher-dimensional bulk spacetime. In this case the extra dimensions may be non-compact [1]. Brane and bulk fields are usually treated as independent degrees of freedom, but in general one should include interactions between brane and bulk fields. For instance, in order to study inhomogeneous perturbations about a brane-world cosmology we need to consistently include bulk metric perturbations coupled to matter perturbations on the brane [2, 3, 4, 5, 6, 7, 8]. Once we include a finite coupling between brane and bulk fields it is no longer possible to think in terms of a brane field without consistently including the associated bulk field configuration, and vice versa.

In this paper we will consider the case of linear coupling between a four-dimensional scalar field on a de Sitter brane and a five-dimensional scalar field in an anti-de Sitter (AdS) bulk spacetime. We will develop an analytic approach based on the resonant scattering modes of the bulk field as has recently been applied to the study of quasinormal modes of the gravitational field about Randall-Sundrum [9] and Einstein-static [10, 11] branes. We identify both evanescent scattering modes (quasinormal modes) of the bulk field, which decay at future null infinity, and normalisable bound states. Our linearly coupled brane and bulk perturbations about a de Sitter brane may be seen as a simplified model of perturbations in the inflaton field driving slow-roll inflation on a brane which are linearly coupled to scalar metric

perturbations in the bulk [12, 13, 14].

Linearly coupled brane and bulk fields on a Minkowski brane have been previously studied in a Minkowski bulk [15, 16] and in an anti-de Sitter (AdS) bulk [16]. In a Minkowski bulk there is always one and only one bound state, and above a critical coupling the bound state describes a tachyonic instability [15]. In an AdS bulk one finds again a tachyonic bound state above a critical coupling, but below the critical coupling there is no bound state [16]. On the other hand we know there is a bound state for a light bulk field in the case of zero coupling in the presence of a de Sitter brane. The spectrum of free bulk modes is qualitatively different in the presence of a de Sitter brane as only modes above a finite mass gap (proportional to the Hubble rate on the brane) can escape to null infinity [17]. We will investigate the existence of bound states with finite coupling between bulk and brane fields in the presence of a de Sitter brane, finding zero, one or two bound states depending upon the parameter values.

We also present a numerical code to solve for the evolution of the bulk field coupled to the scalar field on a moving brane in the bulk spacetime. This is a development of Seahra's numerical code [18] (see also [14, 19, 20, 21, 22]) for bulk perturbations with an arbitrary brane trajectory but no brane coupling, to include coupled degrees of freedom on the brane. We use this to test our analytic results, but we also expect this numerical code to be useful to investigate a wider range of models such as metric perturbations in a bulk spacetime which have a non-trivial coupling to the brane fields and are thus less amenable to analytic study [12, 13, 14].

The layout of the paper is as follows: In Sec. II, we introduce our model and the notation used throughout the paper. Sec. III discusses the spectral solution of the equations of motion and the system's resonant excitations. An effective 4-dimensional description of the model's bound state sector is developed and compared to the full theory in Sec. IV. Direct solution of the wave equations in the time domain via numeric computation is the topic of Sec. V. Finally, Sec. VI is reserved for our conclusions.

^{*}Electronic address: antonio.cardoso@port.ac.uk

[†]Electronic address: kazuya.koyama@port.ac.uk

[‡]Electronic address: andrew.mennim@port.ac.uk

[§]Electronic address: sanjeev.seahra@port.ac.uk

[¶]Electronic address: david.wands@port.ac.uk

II. STATEMENT OF THE PROBLEM

In this section, we describe the model analyzed in this paper. We consider a portion of AdS space \mathcal{M} bounded by a brane $\partial\mathcal{M}_b$. The bulk geometry can be usefully described by two different coordinate systems

$$\begin{aligned} ds_5^2 &= \frac{\ell^2}{z^2}(-dt^2 + d\mathbf{x}^2 + dz^2) \\ &= \left(\frac{H\ell}{\sinh Hy} \right)^2 (-d\tau^2 + e^{2H\tau} d\mathbf{x}^2 + dy^2). \end{aligned} \quad (1)$$

The first set of coordinates (“Poincaré”) are related to the second set (“brane normal”) by

$$Ht = -e^{-H\tau} \cosh Hy, \quad Hz = e^{-H\tau} \sinh Hy. \quad (2)$$

Here H is the Hubble parameter: a positive constant with dimensions $(\text{length})^{-1}$.

The trajectory of the brane in the brane normal coordinates is simply

$$y = y_b = H^{-1} \text{arcsinh } H\ell, \quad (3)$$

which gives the induced line element

$$ds_b^2 = -d\tau^2 + e^{2H\tau} d\mathbf{x}^2 = (H\eta)^{-2} (-d\eta^2 + d\mathbf{x}^2), \quad (4)$$

where we have defined the conformal time η by

$$H\eta = -e^{-H\tau}, \quad \eta < 0. \quad (5)$$

From (4), we see that τ is the proper time on the brane. We can also write down the trajectory of the brane in Poincaré coordinates:

$$t = t_b = \gamma\eta, \quad z = z_b = -\eta H\ell, \quad (6)$$

where

$$\gamma = \sqrt{1 + H^2\ell^2} = \cosh Hy_b. \quad (7)$$

We write the normal vector to the brane and the brane induced metric as

$$n^a \partial_a = \partial_y = (-H\eta)(-H\ell \partial_t + \gamma \partial_z), \quad (8a)$$

$$h_{ab} = g_{ab} - n_a n_b. \quad (8b)$$

Finally, note that our bulk manifold \mathcal{M} corresponds to $y > y_b$, which implies that $t < 0$ and $z > 0$ by the coordinate transformation (2). We assume the \mathbb{Z}_2 symmetry, which implies that the “other” half of the bulk ($y \not> y_b$) is the mirror image of \mathcal{M} .

We consider two massive test scalar fields propagating on this background geometry. One of the fields ϕ exists throughout the bulk, while the other q is confined to the brane. These are governed by the action

$$\begin{aligned} S &= - \int_{\mathcal{M}} (g^{ab} \partial_a \phi \partial_b \phi + m^2 \phi^2) \\ &\quad - \frac{1}{2} \int_{\partial\mathcal{M}_b} (h^{ab} \partial_a q \partial_b q + \mu^2 q^2 + 2\beta \phi q). \end{aligned} \quad (9)$$

The bulk part of the action is twice the usual expression due to the \mathbb{Z}_2 symmetry. The coupling constant β has dimensions of $(\text{length})^{-3/2}$ and can be taken to be positive without loss of generality. The masses of ϕ and q are m and μ , respectively. Variation with respect to each field yields the equations of motion

$$g^{ab} \nabla_a \nabla_b \phi = m^2 \phi, \quad (10a)$$

$$h^{\alpha\beta} \nabla_\alpha \nabla_\beta q = \mu^2 q + \beta \phi_b, \quad (10b)$$

where $h_{\alpha\beta}$ and ∇_α are the intrinsic metric and covariant derivative on $\partial\mathcal{M}_b$, respectively, and ϕ_b is the bulk field evaluated on the brane. The bulk field satisfies the boundary condition

$$(n^a \partial_a \phi)_b = \frac{1}{2} \beta q. \quad (11)$$

In what follows, we will almost always work with the spatial Fourier transforms of the fields

$$\phi(\tau, \mathbf{x}, y) = \int d^3k e^{-i\mathbf{k}\cdot\mathbf{x}} \phi_{\mathbf{k}}(\tau, y), \quad (12a)$$

$$q(\tau, \mathbf{x}) = \int d^3k e^{-i\mathbf{k}\cdot\mathbf{x}} q_{\mathbf{k}}(\tau). \quad (12b)$$

The \mathbf{k} subscript on ϕ and q will be omitted in all the formulae below, with the exception of those in Sec. IV, where we work with the fields in real space.

III. SPECTRAL ANALYSIS

In this section, we seek the solution to the equations of motion for our system (10) via a spectral decomposition of the fields. Our main goal will be to find and classify the resonant modes in the problem by looking at the poles of the scattering matrix. Throughout this section, we use the brane normal (τ, y) coordinates.

A. Canonical wave equations and the scattering matrix

To put the wave equations into canonical form we introduce the re-scaled fields $\tilde{\phi}$ and \tilde{q} , defined by

$$\phi(\tau, y) = e^{-3H\tau/2} (\sinh Hy)^{3/2} \tilde{\phi}(\tau, y), \quad (13a)$$

$$q(\tau) = e^{-3H\tau/2} \tilde{q}(\tau). \quad (13b)$$

Then, the wave equations (10) reduce to

$$[\partial_\tau^2 + k^2 e^{-2H\tau}] \tilde{\phi} = [\partial_y^2 - U(y)] \tilde{\phi}, \quad (14a)$$

$$[\partial_\tau^2 + k^2 e^{-2H\tau}] \tilde{q} = \left[\frac{9}{4} H^2 - \mu^2 \right] \tilde{q} - \beta (H\ell)^{3/2} \tilde{\phi}_b, \quad (14b)$$

where we have defined the potential

$$U(y) = \frac{H^2(15 + 4m^2\ell^2)}{4(\sinh Hy)^2}. \quad (15)$$

The structure of the equations of motion (14) suggest a spectral decomposition of the form

$$\tilde{\phi}(\tau, y) = \int_{-\infty}^{\infty} d\omega T_\omega(\tau) \tilde{\phi}_\omega(y), \quad (16a)$$

$$\tilde{q}(\tau) = \int_{-\infty}^{\infty} d\omega T_\omega(\tau) \tilde{q}_\omega. \quad (16b)$$

Here, $T_\omega(\tau)$ is an eigenfunction of the temporal operator appearing in (14):

$$[\partial_\tau^2 + k^2 e^{-2H\tau}] T_\omega(\tau) = -\omega^2 H^2 T_\omega(\tau). \quad (17)$$

This is satisfied if we take

$$T_\omega(\tau) = \left(\frac{k}{2H}\right)^{i\omega} \left(\frac{H\omega}{2\sinh \pi\omega}\right)^{1/2} J_{-i\omega} \left(\frac{k}{H} e^{-H\tau}\right), \quad (18)$$

where $J_\nu(x)$ is the Bessel function of the first kind. We note that T_ω reduces to a single-frequency plane wave in the limit of large τ ,

$$T_\omega(\tau) \sim \left(\frac{H\omega}{2\sinh \pi\omega}\right)^{1/2} \frac{e^{i\omega H\tau}}{\Gamma(1-i\omega)}, \quad [H\tau \gg \ln k/H]. \quad (19)$$

The normalisation coefficient in (18) has been selected such that

$$\delta(\omega - \omega') = \int_{-\infty}^{+\infty} d\tau T_\omega(\tau) T_{\omega'}^*(\tau). \quad (20)$$

Putting (16) into (14) yields

$$0 = [\partial_y^2 - U(y) + \omega^2 H^2] \tilde{\phi}_\omega, \quad (21a)$$

$$0 = [\omega^2 H^2 + \frac{9}{4} H^2 - \mu^2] \tilde{q}_\omega - \beta(H\ell)^{3/2} \tilde{\phi}_{b\omega}. \quad (21b)$$

The general solution of (21a) is

$$\tilde{\phi}_\omega(y) = a_\omega^+ \tilde{\phi}_\omega^+(y) + a_\omega^- \tilde{\phi}_\omega^-(y), \quad (22a)$$

$$\tilde{\phi}_\omega^+(y) = \mathcal{N}^+ (\sinh Hy)^{1/2} R_{i\omega-1/2}^\alpha(\cosh Hy), \quad (22b)$$

$$\tilde{\phi}_\omega^-(y) = \mathcal{N}^- (\sinh Hy)^{1/2} Q_{i\omega-1/2}^\alpha(\cosh Hy), \quad (22c)$$

where

$$R_\sigma^\alpha(x) = \frac{\pi e^{i\pi\alpha} P_\sigma^\alpha(x) - Q_\sigma^\alpha(x) \sin \pi(\sigma + \alpha) \sec \pi\sigma}{\Gamma(\sigma + 3/2) \Gamma(\sigma + 1/2)},$$

$$\mathcal{N}^\pm = 2e^{-i\pi\alpha} \left(\frac{\pi\omega}{H \sinh \pi\omega}\right)^{1/2} [\Gamma(i\omega + \frac{1}{2} \mp \alpha)]^{\pm 1},$$

$$\alpha = \sqrt{4 + m^2 \ell^2}. \quad (23)$$

Here, $P_\sigma^\alpha(x)$ and $Q_\sigma^\alpha(x)$ are associated Legendre functions [23, 8.7]. The coefficients \mathcal{N}^\pm have been selected such that when we use the standard asymptotic expansions [23, 8.776], we have

$$T_\omega(\tau) \tilde{\phi}_\omega^\pm(y) \sim e^{iH\omega(\tau \pm y)},$$

$$[H\tau \gg \ln k/H \text{ and } Hy \gg 1]. \quad (24)$$

Hence, $\tilde{\phi}$ reduces to a superposition of incoming and outgoing plane waves in the ‘‘asymptotic region’’ defined in the square brackets; i.e., far into the future and far from the brane.

We have yet to enforce the boundary condition (11). In terms of the mode decomposition, this reads

$$\left[\partial_y \tilde{\phi}_\omega + \frac{3}{2} \gamma (H\ell)^{-1} \tilde{\phi}_\omega\right]_b = \frac{1}{2} \beta (H\ell)^{-3/2} \tilde{q}_\omega. \quad (25)$$

When (22) is substituted into (21b) and (25), we obtain a homogeneous system of two equations linear in $(a_\omega^\pm, \tilde{q}_\omega)$ which can be solved for the amplitude ratios $a_\omega^\pm / \tilde{q}_\omega$. The derivatives of Legendre functions appearing in this system can be simplified using recurrence relations [23, 8.732].

We define the scattering matrix (i.e., reflection coefficient) \mathcal{S}_ω as the ratio of outgoing to ingoing flux in the asymptotic region (cf. Eq. 24) at a particular frequency ω . Explicitly, we obtain

$$\mathcal{S}_\omega = \frac{a_\omega^-}{a_\omega^+} = -\frac{1}{\omega \Gamma^2(i\omega)} \frac{\mathcal{N}^+}{\mathcal{N}^-} \left[\frac{\cos \pi(\alpha + i\omega)}{\sinh \pi\omega} + i\pi e^{i\pi\alpha} \frac{c_+ P_{i\omega+1/2}^\alpha(\gamma) + c_- P_{i\omega-1/2}^\alpha(\gamma)}{c_+ Q_{i\omega+1/2}^\alpha(\gamma) + c_- Q_{i\omega-1/2}^\alpha(\gamma)} \right], \quad (26)$$

where

$$c_+ = \left(\omega^2 + \frac{9}{4} - \frac{\mu^2}{H^2}\right) \left(\alpha - i\omega - \frac{1}{2}\right), \quad (27a)$$

$$c_- = \frac{\ell\beta^2}{2H^2} + i\gamma \left(\omega^2 + \frac{9}{4} - \frac{\mu^2}{H^2}\right) \left(\omega + \frac{3}{2}i\right). \quad (27b)$$

Before moving on, we should mention cases for which (26) is not a valid expression for the scattering matrix:

$$i\omega - 1/2 \pm \alpha \notin \mathbb{Z}, \quad i\omega \notin \mathbb{Z}, \quad (28)$$

where \mathbb{Z} represents the integers. The first of these restrictions is in place to ensure that the mode functions $\tilde{\phi}_\omega^\pm$ are linearly independent [23, 8.707], while the second is required for the asymptotic expressions (24) to be applicable [23, 8.776]. When ω is real, both conditions are automatically satisfied.

B. Resonances

Intuitively, a resonance of a given system is a mode of oscillation where the response (‘‘output’’) is maximised relative to the stimulus (‘‘input’’). In scattering theory, this implies that the outgoing flux associated with a resonant mode completely dominates the ingoing flux. This leads to the formal definition of a resonant excitation: A mode whose frequency corresponds to a pole of the scattering matrix \mathcal{S}_ω when ω is continued into the complex plane [11, 24, 25, 26]. The physical importance of these resonant modes is that they describe the dominant

behaviour of any given system, regardless of the choice of initial conditions. In this context, we expect that the late time behaviour of the brane and bulk fields to be well approximated by resonant solutions irrespective of the configuration on some initial data hypersurface. In this subsection, we study the poles of \mathcal{S}_ω in some detail.

1. General properties of quasinormal modes

When the scattering matrix (26) is continued into the complex plane, one discovers that it has a number of poles on the imaginary ω axis that violate the restrictions (28). Since the scattering matrix itself is undefined at these locations, these poles are ignorable and we omit them from the subsequent discussion. We can show that all of the physical poles that remain correspond to roots of \mathcal{R}_ω , where

$$\begin{aligned} \mathcal{R}_\omega &= \left(\frac{\mu^2}{H^2} - \omega^2 - \frac{9}{4} \right) \left(\alpha - i\omega - \frac{1}{2} \right) Q_{i\omega + \frac{1}{2}}^\alpha(\gamma) \\ &+ \left[\gamma \left(i\omega - \frac{3}{2} \right) \left(\frac{\mu^2}{H^2} - \omega^2 - \frac{9}{4} \right) - \frac{\ell\beta^2}{2H^2} \right] Q_{i\omega - \frac{1}{2}}^\alpha(\gamma). \end{aligned} \quad (29)$$

This condition that $\mathcal{R}_\omega = 0$ is the same as demanding that a particular mode function satisfies the boundary condition at the brane and is a purely outgoing wave in the asymptotic future; i.e., $a_\omega^+ = 0$. Hence, the resonant states we have defined here are akin to the quasinormal modes of black hole perturbation theory [26]. In Fig. 1, we show a plot of $|\mathcal{R}_\omega^{-1}|$ as a function of complex frequency for a certain choice of parameters.

It is useful to note that the full spatial and temporal dependance of a resonant solution for the canonical and physical bulk fields are

$$\tilde{\phi}_\omega^R(\tau, y) = T_\omega(\tau) \tilde{\phi}_\omega(y), \quad (30a)$$

$$\phi_\omega^R(\tau, y) = e^{-3H\tau/2} (\sinh Hy)^{3/2} T_\omega(\tau) \tilde{\phi}_\omega(y), \quad (30b)$$

respectively. In both cases, ω is a root of \mathcal{R}_ω . The asymptotic behaviour of these resonant solutions is crucial to the discussion below. We have for late times

$$\lim_{H\tau \rightarrow \infty} |\tilde{\phi}_\omega^R(\tau, y)| \propto e^{-\Gamma H\tau}, \quad (31a)$$

$$\lim_{H\tau \rightarrow \infty} |\phi_\omega^R(\tau, y)| \propto e^{-(\Gamma+3/2)H\tau}, \quad (31b)$$

while far from the brane, we obtain

$$\lim_{Hy \rightarrow \infty} |\tilde{\phi}_\omega^R(\tau, y)| \propto e^{\Gamma Hy}, \quad (31c)$$

$$\lim_{Hy \rightarrow \infty} |\phi_\omega^R(\tau, y)| \propto e^{(\Gamma+3/2)Hy}, \quad (31d)$$

where $\Gamma = \text{Im } \omega$.

We can use this asymptotic behaviour to derive a useful result for resonances with $\text{Im } \omega < 0$. We multiply (21a)

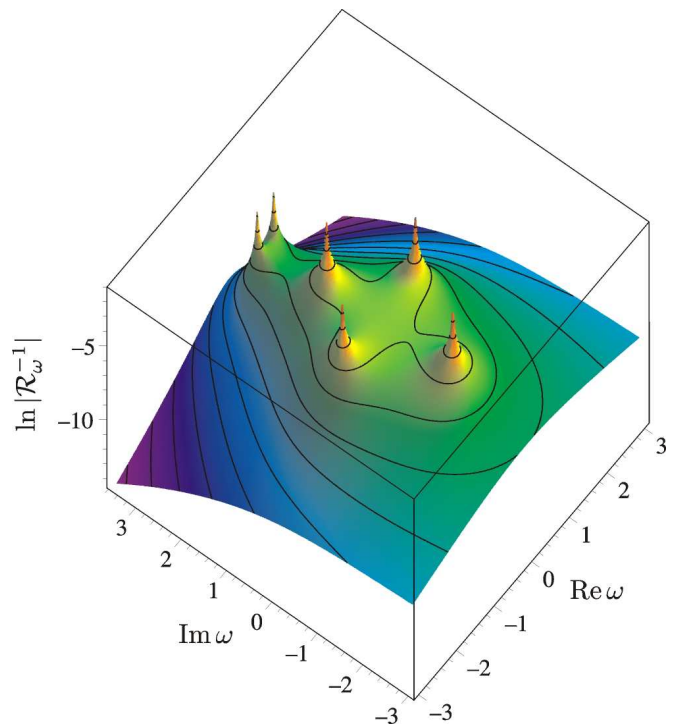


FIG. 1: An example of the distribution of zeros of \mathcal{R}_ω in the complex frequency plane. The vertical axis is $\ln |\mathcal{R}_\omega^{-1}|$, so the tall spikes represent poles of the scattering matrix. For this plot, we have taken $\beta\ell^{3/2} = 1.00$, $m\ell = 3.34$, $H\ell = 1.37$ and $\mu\ell = 1.00$.

by $\tilde{\phi}_\omega^*$ and integrate over y . This yields

$$- \left[\tilde{\phi}_\omega^* \tilde{\phi}'_\omega \right]_b = \int_{y_b}^{\infty} dy \left\{ |\tilde{\phi}'_\omega|^2 + [U - \omega^2 H^2] |\tilde{\phi}_\omega|^2 \right\}, \quad (32)$$

where we have integrated by parts and made use of the fact that $\tilde{\phi}_\omega$ vanishes strongly as $y \rightarrow \infty$ if $\text{Im } \omega < 0$. The lefthand side can be expanded using (21b) and the boundary condition (25). Then, taking the imaginary part of (32), we get

$$0 = \text{Im}(\omega^2) \left[|\tilde{q}_\omega|^2 + 2(H\ell)^3 \int_{y_b}^{\infty} dy |\tilde{\phi}_\omega|^2 \right]. \quad (33)$$

Since the quantity inside the square brackets is manifestly nonzero, we are led to the conclusion $\text{Im}(\omega^2) = 0$. But, we also have that $\text{Im } \omega \neq 0$, from which it follows that $\text{Re } \omega = 0$. That is, any resonant frequencies ω satisfying $\mathcal{R}_\omega = 0$ in the lower half of the complex plane must lie on the imaginary axis.

2. Classification of resonances

We now turn to the classification of resonant modes with complex frequency. One important way of discriminating between different classes of resonance is

the asymptotic behaviour articulated in Eq. (31). Another categorization scheme involves assigning a ‘‘Kaluza-Klein’’ mass ρ to each resonance, which is implicitly defined by noting that ϕ_ω^R satisfies the Klein-Gordon equation on the brane

$$-\rho^2 \phi_\omega^R = (\partial_\tau^2 + 3H \partial_\tau + k^2 e^{-2H\tau}) \phi_\omega^R, \quad (34)$$

where the field mass is

$$\rho^2 = H^2 \left(\omega^2 + \frac{9}{4} \right). \quad (35)$$

Note that for $\text{Im } \omega < 0$, ρ will be purely real or imaginary. On the other hand, if $\text{Im } \omega > 0$ the mass will be complex in general. Finally, we can also classify resonances based on whether or not they are normalisable under the Klein-Gordon inner product:

$$(\phi, \psi)_{\text{KG}} = \frac{1}{V_3} \int_{\Sigma_\tau} t^a (\phi^* \partial_a \psi - \psi \partial_a \phi^*), \quad (36)$$

where Σ_τ is the spacelike 4-surface of constant τ and t^a is its future directed normal vector. We apply a box-normalization of volume V_3 for the spatial 3-manifold. Consider the norm of ϕ_ω^R

$$(\phi_\omega^R, \phi_\omega^R)_{\text{KG}} \propto \int_{y_b}^{\infty} dy \frac{|\phi_\omega^R|^2}{(\sinh Hy)^3} \propto \int_{y_b}^{\infty} dy |\tilde{\phi}_\omega^R|^2. \quad (37)$$

Hence, ϕ_ω^R is normalisable if $\tilde{\phi}_\omega^R$ is square integrable over y .

Armed with these definitions, we can delineate states into three categories:

Scattering states: These are resonances with $\text{Im } \omega > 0$. For these modes, both $\tilde{\phi}_\omega^R$ and ϕ_ω^R vanish at late times. Conversely, both states also diverge for large y , and the Klein-Gordon norm $(\phi_\omega^R, \phi_\omega^R)_{\text{KG}}$ diverges. Hence, these are *not* conventional bound states. This spatial divergence does not mean that scattering states are unphysical, since they are well behaved if the limits $\tau \rightarrow \infty$ and $y \rightarrow \infty$ are taken simultaneously. Scattering states are akin to quasinormal modes in black hole perturbation theory in that they are never observed at spatial infinity, only future null infinity. The Kaluza-Klein mass of scattering states is generally complex.

Overdamped bound states: These have $-3/2 < \text{Im } \omega < 0$ which implies $\text{Re } \omega = 0$. At late times, the canonical field $\tilde{\phi}_\omega^R$ blows-up while the physical field ϕ_ω^R is exponentially damped. These modes are normalisable under the Klein-Gordon product since $(\phi_\omega^R, \phi_\omega^R)_{\text{KG}}$ is finite. The Kaluza-Klein mass of these modes is real since $\rho^2 > 0$. Because ϕ_ω^R vanishes in the infinite future and is normalisable, we call these modes ‘‘overdamped bound states’’.

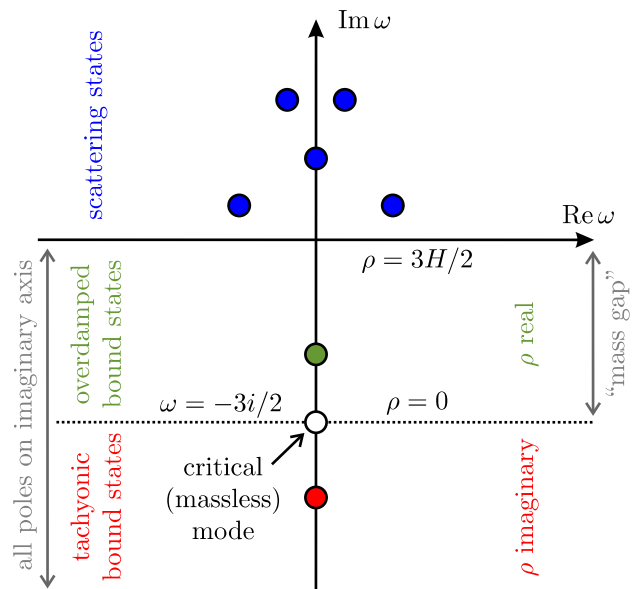


FIG. 2: Different classes of possible resonances. The circles indicate poles of the scattering matrix.

Tachyonic bound states: These have $\text{Im } \omega < -3/2$ and $\text{Re } \omega = 0$. They are normalisable and diverge at late times. In this case, the Kaluza-Klein mass is imaginary $\rho^2 < 0$, which is why we call these modes ‘‘tachyonic bound states’’.

We summarize this classification scheme in Fig. 2. We have indicated the ‘‘mass gap’’ between $\rho = 0$ and $\rho = 3H/2$ familiar from the analysis of uncoupled bulk fields about de Sitter branes.

3. Critical coupling and the massless mode

For any choice of μ , m , $H\ell > 1$, it is always possible to choose the coupling parameter $\beta = \beta_{\text{crit}} \in \mathbb{R}$ such that there is one resonance with frequency $\omega = -3i/2$ and Kaluza-Klein mass $\rho = 0$. To see this, we substitute $\omega = -3i/2$ in $\mathcal{R}_\omega = 0$ and solve for β_{crit} :

$$\beta_{\text{crit}} = \frac{\mu \sqrt{2(\alpha - 2)}}{\ell^{1/2}} \left[\frac{Q_2^\alpha(\gamma)}{Q_1^\alpha(\gamma)} \right]^{1/2}. \quad (38)$$

Note that a fundamental property of the associated Legendre function of the second kind is that [23, 8.783]

$$e^{-i\pi\alpha} Q_\sigma^\alpha(\gamma) > 0 \text{ for all } \sigma > -\frac{3}{2}, \alpha > -\frac{1}{2}, \gamma > 1. \quad (39)$$

From this it follows that β_{crit} is real for all possible parameter choices; i.e., it is always possible to select the coupling such that at least one resonance is massless. Note also that $\beta_{\text{crit}} = 0$ when either m or μ is zero.

The qualitative behaviour of this massless mode at late times is the same as a massless scalar propagating in 4-dimensional de Sitter: Namely, the physical field amplitude ϕ_ω^R is frozen (conserved) on superhorizon scales.

4. Bound state resonances

In Fig. 3, we track the resonant roots of \mathcal{R}_ω through the complex plane as a function of the coupling $\beta/\beta_{\text{crit}}$ for particular values of the masses. Here and in Sec. V C below, the roots are found numerically using Newton's method. We see that there are bound states for all couplings, but there is only a tachyonic mode for supercritical ($\beta > \beta_{\text{crit}}$) coupling. Furthermore, in the small coupling regime, we see two overdamped bound states. The behaviour of the resonant frequencies for a different choice of parameters is shown in Fig. 4. In this scenario, no bound state even exists for small coupling. In both cases, we see that the fundamental mode goes from overdamped to tachyonic as the coupling is increased through the critical value. There is no mode mixing in general at this coupling, although at other couplings it is possible for modes to merge or bifurcate (for example, around $\beta \sim 0.6 \times \beta_{\text{crit}}$ in Fig. 3). Our purpose in this subsection is to understand some of this bound state behaviour in terms of the general properties of \mathcal{R}_ω .

Massive bulk and brane fields We are only interested in the bound states, so we set

$$\omega = -i(\lambda + \frac{3}{2}), \quad \lambda > -\frac{3}{2}. \quad (40)$$

If the Kaluza-Klein mass of a resonance corresponding to a given value of λ is ρ_λ , then we have

$$\rho_\lambda^2 = -H^2\lambda(\lambda + 3) = \begin{cases} \text{positive,} & \lambda \in [-\frac{3}{2}, 0), \\ \text{negative,} & \lambda \in (0, \infty); \end{cases} \quad (41)$$

i.e., any bound state with $\lambda > 0$ is a tachyon.

Assuming that $\alpha > 2$ and $\mu > 0$, and mindful of (39), we can re-write the resonance condition as

$$(\beta/\beta_{\text{crit}})^2 = \mathcal{Z}(\lambda), \quad (42)$$

where

$$\mathcal{Z}(\lambda) = \frac{1}{(\alpha - 2)} \frac{Q_1^\alpha(\gamma)}{Q_2^\alpha(\gamma)} \left(1 - \frac{\rho_\lambda^2}{\mu^2} \right) \times \left[(\lambda + \alpha + 1) \frac{Q_\lambda^\alpha(\gamma)}{Q_{\lambda+1}^\alpha(\gamma)} - \gamma(\lambda + 3) \right]. \quad (43)$$

Empirically, we find that for all $\alpha > 2$, $\mu > 0$ and $\gamma > 1$, the continuously differentiable function $\mathcal{Z}(\lambda) \in \mathbb{R}$ has the following properties:

- Over the interval $\lambda \in [0, \infty)$, $\mathcal{Z}(\lambda)$ monotonically increases from 1 to ∞ . Therefore, there always exists one and only one tachyonic bound state for supercritical coupling $\beta > \beta_{\text{crit}}$.
- In the interval $\lambda \in [-3/2, 0]$, $\mathcal{Z}(\lambda)$ has at most one local minimum and no local maxima. Therefore, for any choice of parameters we can have at most two bound state resonances.

- The absolute minimum of $\mathcal{Z}(\lambda)$ for $\lambda \in [-3/2, \infty)$ is always less than unity, but not necessarily less than zero. Therefore, it is possible to select parameters such that there are no bound states at all. Such situations will always have subcritical coupling $\beta < \beta_{\text{crit}}$.

We reiterate that these conclusions are only valid with both fields have finite mass.

From these comments, we can deduce that a necessary (but not sufficient) condition for the existence of two bound states is

$$\mathcal{Z}(-3/2) > 0 \text{ and } \mathcal{Z}'(-3/2) < 0. \quad (44)$$

By direct sampling of the $(\mu/H, m\ell, H\ell)$ parameter space, we have numerically determined that these conditions hold if and only if

$$\mu/H < 3/2 \text{ and } m^2/H^2 < \hat{m}_{\text{thres}}^2(H\ell). \quad (45)$$

Here, the dimensionless threshold mass $\hat{m}_{\text{thres}}^2(H\ell)$ is obtained numerically and shown in Fig. 5. We will see in Sec. III C 1 below, that the second inequality in (45) is a necessary and sufficient condition for there to exist a bound state of ϕ at zero coupling.

Massless bulk field The situation is somewhat different when either m or μ is set to zero. For the sake of brevity, we only mention the case of the massless bulk field here. When $\alpha = 2$, the condition for bound states is

$$\beta^2/H^3 = \mathcal{Y}(\lambda), \quad (46)$$

where,

$$\mathcal{Y}(\lambda) = \frac{2\rho_\lambda^2(\rho_\lambda^2 - \mu^2)}{H^4} \left[-\frac{Q_{\lambda+1}^1(\gamma)}{Q_{\lambda+1}^2(\gamma)} \right]. \quad (47)$$

The function $\mathcal{Y}(\lambda) \in \mathbb{R}$ is continuously differentiable for $\lambda > -3/2$, and has the following properties:

- $\mathcal{Y}(\lambda)$ monotonically increases from 0 to ∞ for $\lambda \in [0, \infty)$. Therefore, there always exists one and only one tachyonic bound state for any nonzero coupling $\beta > 0$.
- The sign of \mathcal{Y} at $\lambda = -3/2$ satisfies $\text{sgn}[\mathcal{Y}(-3/2)] = \text{sgn}[\frac{3}{2}H - \mu]$. Therefore, in addition to the ubiquitous tachyonic mode, one can have an overdamped bound state if and only if the mass of the brane field lies in the mass gap $\mu < \frac{3}{2}H$.
- $\mathcal{Y}(\lambda)$ has at most one local extremum for $\lambda \geq -3/2$. If this extremum exists, it must be a minimum inside $[-3/2, 0]$. Hence, we can either have one tachyonic and one overdamped resonance, or one tachyonic resonance only.

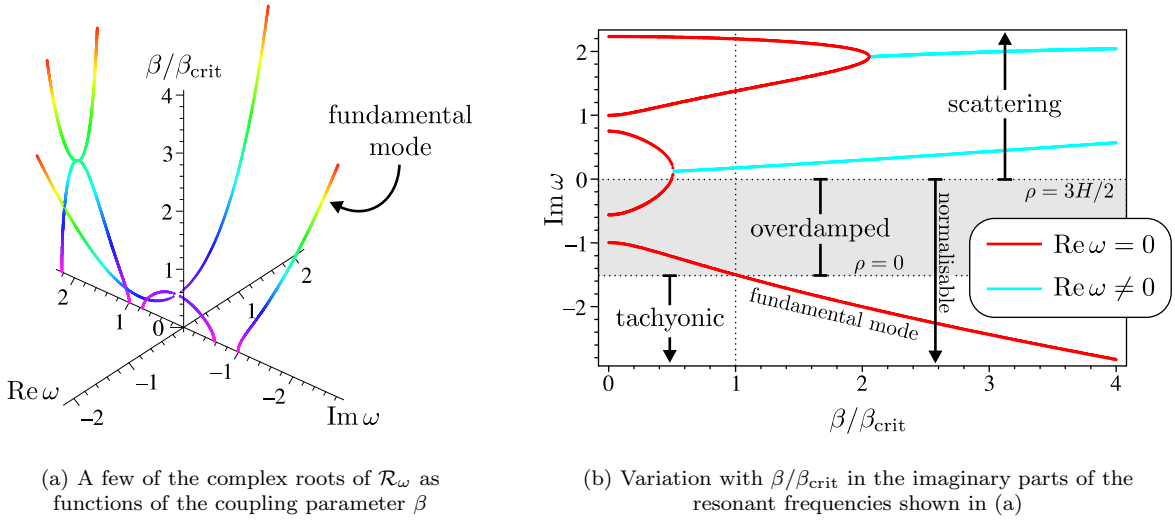


FIG. 3: The least-damped resonant frequencies of the system when $\mu\ell = 1.40$, $m\ell = 2.37$ and $H\ell = 1.25$. This particular example illustrates the generic feature of our model: a tachyonic resonance only exists for supercritical ($\beta > \beta_{\text{crit}}$) coupling. Note that all resonances with $\text{Im}\omega < 0$ have $\text{Re}\omega = 0$, as expected. Also note that the two $\beta = 0$ resonances $\omega = \pm 0.998i$ are modes for which the bulk field vanishes $\phi_\omega^{\text{R}} = 0$ (i.e. these are pure q modes), while the other modes have a vanishing brane mode $q_\omega^{\text{R}} = 0$. The “fundamental mode” has been identified as the resonance with the smallest imaginary part, which is expected to dominate the late time behaviour of numeric simulations (cf. Sec. V C).

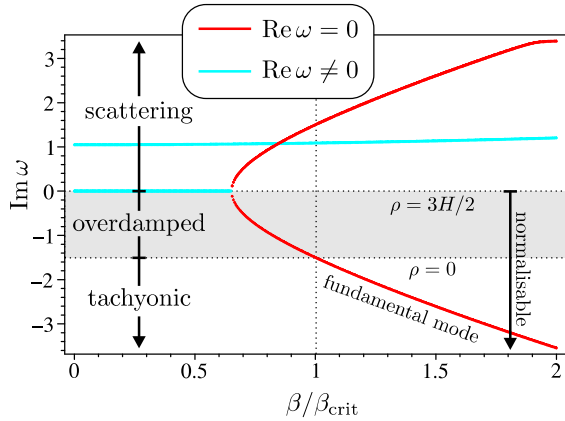


FIG. 4: Variation in the imaginary parts of the least-damped resonant frequencies with coupling when $\mu\ell = 0.40$, $m\ell = 2.1$ and $H\ell = 0.20$. In contrast to Fig. 3, there is no bound state at small coupling. For $\beta/\beta_{\text{crit}} \gtrsim 0.65$, there is a single bound state that is overdamped or tachyonic for subcritical or supercritical coupling, respectively.

C. Limiting cases

In this subsection, we consider the resonance condition $\mathcal{R}_\omega = 0$ in various limits and hence recover several results from the literature.

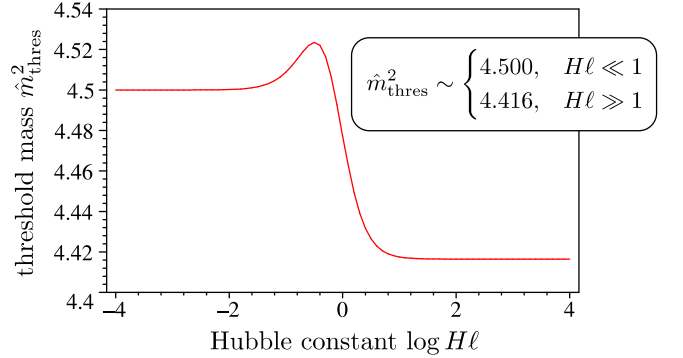


FIG. 5: The threshold mass as obtained from numeric calculations. The condition $m^2/H^2 < \hat{m}_{\text{thres}}^2(H\ell)$ is necessary for the existence of two bound states when the coupling is nonzero. In Sec. III C 1, we also see that this condition is necessary and sufficient for the existence of a bound state of the bulk field at zero coupling.

1. Zero coupling

We first consider the zero coupling limit of the model $\beta = 0$. It is useful to define

$$\mathcal{R}_\omega^{(\phi)} = (\alpha - i\omega - 1/2) Q_{i\omega+1/2}^\alpha(\gamma) + \gamma(i\omega - 3/2) Q_{i\omega-1/2}^\alpha(\gamma), \quad (48a)$$

$$\mathcal{R}_\omega^{(q)} = \mu^2/H^2 - \omega^2 - 9/4. \quad (48b)$$

In terms of these functions, we find that $\mathcal{R}_\omega = 0$ implies

$$\mathcal{R}_\omega^{(\phi)} = 0 \text{ or } \mathcal{R}_\omega^{(g)} = 0, \quad [\beta = 0]. \quad (49)$$

Going back to the analysis of Sec. III A, we can show that if either the first or second condition holds, then $\tilde{q}_\omega^{\text{R}}(\tau) = 0$ or $\tilde{\phi}_\omega^{\text{R}}(\tau, y) = 0$, respectively. In other words, each condition represents the resonances of one field decoupled from the other. The brane field resonances are trivial

$$\omega = \pm \sqrt{\mu^2/H^2 - 9/4} \Rightarrow \rho^2 = \mu^2; \quad (50)$$

that is, these modes oscillate with the natural frequency of the brane oscillator in isolation and have a Kaluza-Klein mass equal to μ .

Using an identity [23, 8.739] and recurrence relations [23, 8.73], the bulk resonance condition $\mathcal{R}_\omega^{(\phi)} = 0$ can be re-written as

$$\begin{aligned} 0 &= \zeta(\alpha - 2)P_{\alpha-1/2}^{-i\omega}(\zeta) + (i\omega - \alpha + \frac{1}{2})P_{\alpha-3/2}^{-i\omega}(\zeta) \\ &= (i\omega + \alpha + \frac{1}{2})P_{\alpha+1/2}^{-i\omega}(\zeta) - \zeta(\alpha + 2)P_{\alpha-1/2}^{-i\omega}(\zeta), \end{aligned} \quad (51)$$

where $\zeta = \gamma/(H\ell)$. These match the various bound state criteria obtained for a massive scalar field about a de Sitter brane in Refs. [27, 28, 29] (up to trivial differences in notation).

As in Sec. III B 4 above, we can substitute in $\omega = -i(\lambda + \frac{3}{2})$ into the bulk resonance condition $\mathcal{R}_\omega^{(\phi)} = 0$ to derive a criterion for bound state resonances of ϕ at zero coupling. This is

$$0 = \mathcal{X}(\lambda) = \frac{Q_{\lambda+2}^\alpha(\gamma)}{Q_{\lambda+1}^\alpha(\gamma)} - \frac{\gamma\lambda}{\lambda + 2 - \alpha}, \quad \lambda > -\frac{3}{2}. \quad (52)$$

One can confirm that $\mathcal{X}(\lambda) \in \mathbb{R}$ is monotonically increasing for $\lambda > -3/2$ and positive definite for $\lambda > 0$. Therefore, a de-coupled massive bulk field can exhibit at most one bound state, and this must be an overdamped resonance. Furthermore, a necessary and sufficient condition for the existence of such a bound state is that $\mathcal{X}(-3/2) < 0$, which we have numerically determined is equivalent to

$$m^2/H^2 < \hat{m}_{\text{thres}}^2(H\ell), \quad (53)$$

where the function $\hat{m}_{\text{thres}}^2(H\ell)$ is shown in Fig. 5. In other words, if the bulk field is too heavy compared with the Hubble scale, it cannot be effectively localised near the brane.

Finally, setting the bulk field mass to zero (i.e. $\alpha = 2$) in (48a) yields that

$$0 = (\omega + \frac{3}{2}i)(\omega - \frac{3}{2}i)Q_{i\omega-1/2}^1(\gamma). \quad (54)$$

In this case there is always a critical bound state with $\omega = -3i/2$, which is usually called the zero mode; i.e.,

$$\text{zero mode} \Leftrightarrow \omega = -3i/2, \quad m = 0, \quad \beta = 0. \quad (55)$$

One can confirm that for the zero mode, the resonant solution is y -independent

$$\partial_y \phi^{\text{R}}(\tau, y) = 0. \quad (56)$$

This fact will be useful in the interpretation of the effective 4-dimensional theory in Sec. IV.

2. Perturbed zero mode

Since the coefficients in front the Legendre functions in (29) vanish when $m = 0$ and $\omega = -3i/2$, it is possible to linearise the resonance condition about the zero mode solution (55). In particular, we can take

$$|\omega + \frac{3}{2}i| \ll 1, \quad m\ell \ll 1, \quad \ell\beta^2 \ll \min(\mu^2, H^2), \quad (57)$$

expand \mathcal{R}_ω to linear order in small quantities, and solve for ω . Substituting this solution into (35), we obtain

$$\begin{aligned} \delta\rho_{\text{zero}}^2 &\sim m^2g(H\ell) - \ell^{-1}\mu^{-2}\beta^2f(H\ell) \\ &\sim m^2g(H\ell)(1 - \beta^2/\beta_{\text{crit}}^2), \end{aligned} \quad (58)$$

where $\delta\rho_{\text{zero}}$ is the small Kaluza-Klein mass that the zero mode acquires when either m or β is nonzero. Here, we have defined

$$f(x) = \left[\sqrt{x^2 + 1} - x^2 \ln \left(\frac{1 + \sqrt{x^2 + 1}}{x} \right) \right]^{-1}, \quad (59a)$$

$$g(x) = \frac{1}{2}f(x)\sqrt{x^2 + 1} - \frac{3}{4}x^2, \quad (59b)$$

and made use of the limiting values of the critical coupling (38) for $m\ell \ll 1$:

$$\beta_{\text{crit}}^2 \sim \ell m^2 \mu^2 \frac{g(H\ell)}{f(H\ell)} \rightarrow \begin{cases} \frac{1}{2}m^2\mu^2\ell, & H\ell \ll 1, \\ \frac{2}{5}m^2\mu^2H^{-1}, & H\ell \gg 1, \end{cases} \quad (60)$$

as well as explicit representations of the Legendre functions with integral indices [23, 8.827]. We see that the mass of the bulk field tends to increase the squared mass of the zero mode into the overdamped region, while the coupling tends to decrease it into the tachyonic regime. We also see that supercritical coupling $\beta > \beta_{\text{crit}}$ explicitly leads to a tachyonic mode $\delta\rho_{\text{zero}}^2 < 0$. For reference, we note the limiting behaviour of $\delta\rho_{\text{zero}}$ when $H\ell$ takes on extreme values:

$$\delta\rho_{\text{zero}}^2 \rightarrow \begin{cases} \frac{1}{2}m^2 - \ell^{-1}\mu^{-2}\beta^2, & H\ell \ll 1, \\ \frac{3}{5}m^2 - \frac{3}{2}\mu^{-2}H\beta^2, & H\ell \gg 1. \end{cases} \quad (61)$$

Note that for the perturbed zero mode to be a bound state, we need

$$\delta\rho_{\text{zero}} < 3H/2 \Rightarrow m/H < \sqrt{3}/2, \quad [H\ell \ll 1]. \quad (62)$$

This matches the small $H\ell$ behaviour of the bound state condition $m^2/H^2 < \hat{m}_{\text{thres}}^2$, where \hat{m}_{thres}^2 is shown in Fig. 5. There is no conclusion to be drawn in the other extreme, because the conditions (57) imply $\delta\rho_{\text{zero}}/H \ll 1$ for $H\ell \gg 1$; i.e., the perturbed zero mode is always a bound state.

We note that the expression (58) for $\delta\rho_{\text{zero}}$ closely resembles that obtained by Langlois and Sasaki [29], who studied a massive bulk scalar with a brane-localized self-coupling. Their model was governed by the action

$$S_{\text{LS}} = - \int_{\mathcal{M}} (g^{ab} \partial_a \phi \partial_b \phi + m^2 \phi^2) - \int_{\partial\mathcal{M}_b} \frac{\chi}{\ell} \phi^2, \quad (63)$$

where χ is a dimensionless constant parameter. Their results for the perturbative zero mode mass match ours if we make the identification

$$\chi = -\frac{1}{2}\mu^{-2}\beta^2\ell. \quad (64)$$

Hence, under the conditions (57), our system behaves like a massive bulk scalar field with a constant brane self-coupling.

3. Low energy

The low energy limit of the model is defined by

$$H\ell \ll 1, \quad \gamma \sim 1, \quad [\ell \text{ finite}]. \quad (65)$$

Consider the temporal eigenvalue equation (17) in this regime:

$$(\partial_\tau^2 + k^2)T_\omega(\tau) = -\omega_{\text{phys}}^2 T_\omega(\tau), \quad \omega_{\text{phys}} = \omega H, \quad (66)$$

where we have identified the dimensionful physical frequency ω_{phys} . When we take the limit $H\ell \rightarrow 0$, we want to ensure that the physical frequency is finite. Hence, we define $\hat{\rho}^2/\ell^2$ to be the *finite* eigenvalue of $(\partial_\tau^2 + k^2)$:

$$\hat{\rho} = \omega H\ell = \ell\omega_{\text{phys}}, \quad \lim_{H\ell \rightarrow 0} |\hat{\rho}| < \infty, \quad \lim_{H\ell \rightarrow 0} |\omega| = \infty. \quad (67)$$

In terms of $\hat{\rho}$, the solution of (66) is

$$T_\omega(\tau) = e^{i\varpi\tau/\ell}, \quad \varpi = \sqrt{\hat{\rho}^2 + k^2\ell^2}. \quad (68)$$

To find the resonant modes in this case, our strategy will be to take the limit of $\mathcal{R}_\omega = 0$ when $\gamma \rightarrow 1$, $H\ell \ll 1$, $|\omega| \gg 1$, and ω real. To avoid branch cut ambiguities, we put $\hat{\rho} \rightarrow \hat{\rho} - i0^+$ with $\hat{\rho} \in \mathbb{R}$. The resulting expression can then be continued into the $\hat{\rho}$ complex plane.

Consider the following integral representation of the associated Legendre function [23, 8.711(4)]:

$$Q_\sigma^\alpha(\gamma) = \frac{e^{i\pi\alpha}\Gamma(\sigma+1)}{\Gamma(\sigma-\alpha+1)} \int_0^\infty \frac{dt \cosh at}{(\gamma + \sqrt{\gamma^2 - 1} \cosh t)^{\sigma+1}},$$

[$\gamma > 1$, $\text{Re}(\sigma - \alpha) > -1$, and $-\sigma \neq 1, 2, \dots$]. (69)

Now, if we assume $\gamma \rightarrow 1$ and $\sigma = i\omega \pm 1/2 \sim i(\hat{\rho} - i0^+)(H\ell)^{-1}$ in the integrand of (69), we obtain

$$Q_{i\omega+1/2}^\nu(\gamma) \sim \frac{e^{i\pi\nu}\Gamma(i\omega+3/2)}{\Gamma(i\omega-\nu+3/2)} \times \underbrace{\int_0^\infty dt \exp[-i(\hat{\rho} - i0^+) \cosh t] \cosh \nu t}_{= -\frac{1}{2}i\pi e^{-i\nu\pi/2} H_\nu^{(2)}(\hat{\rho} - i0^+)}, \quad (70)$$

where the integral [23, 3.457(4)] has been evaluated assuming the principal branch of the Hankel functions $H_\nu^{(1,2)}(z)$ [23, 8.476(7)] and fundamental definitions [23,

8.407]. Using (67)–(70), a recurrence relation [23, 8.734(4)], and expanding to leading order in $H\ell$, we obtain the resonant condition for low energies:

$$0 = \left[\frac{1}{2}\beta^2\ell^3 + (\alpha - 2)(\hat{\rho}^2 - \mu^2\ell^2) \right] H_\alpha^{(2)}(\hat{\rho} - i0^+) - \hat{\rho}(\hat{\rho}^2 - \mu^2\ell^2) H_{\alpha-1}^{(2)}(\hat{\rho} - i0^+) + \mathcal{O}(H\ell). \quad (71)$$

This matches the result obtained in Koyama et al. [16] if one takes into account different conventions for the field time dependence and an implicit choice of integration contour for the inverse Fourier transform. Note that in this limit, the Kaluza-Klein mass (35) of a given resonance is

$$\rho^2 = \frac{\hat{\rho}^2}{\ell^2} + \frac{9H^2}{4} \xrightarrow{H\ell \rightarrow 0} \frac{\hat{\rho}^2}{\ell^2}. \quad (72)$$

Hence, the critical massless mode corresponds to $\hat{\rho} = 0$. As before, this mode is a resonance if β equals some critical value

$$\beta_{\text{crit}} = \mu\ell^{-1/2} \sqrt{2(\alpha - 2)}. \quad (73)$$

As discussed in detail in Ref. [16], bound states in this limit correspond to resonances with $\hat{\rho}$ on the negative imaginary axis. One can only have a bound state for supercritical coupling, and that unique bound state is necessarily tachyonic.

Eq. (71) can be linearised about the resonance (55), resulting in the mass perturbation of the zero mode:

$$\delta\rho_{\text{zero}}^2 \sim \frac{1}{2}m^2 - \frac{1}{\mu^2\ell}\beta^2 \sim \frac{1}{2}m^2 \left(1 - \frac{\beta^2}{\beta_{\text{crit}}^2} \right), \quad (74)$$

where the last approximation comes from expanding the critical coupling about $m = 0$. One can confirm that this reproduces the $H\ell \ll 1$ limit of Eq. (58).

We can also take the limit of (71) in the case of a flat bulk

$$\ell \rightarrow \infty, \quad \hat{\rho} = \rho\ell \rightarrow \infty, \quad m\ell \sim \alpha \rightarrow \infty, \quad (75)$$

by making use of the following fact [16]:

$$\frac{\hat{\rho} H_{\alpha-1}^{(2)}(\hat{\rho})}{H_\alpha^{(2)}(\hat{\rho})} + 2 - \alpha \xrightarrow{\frac{(\hat{\rho}, \alpha)}{\infty}} -\sqrt{m^2\ell^2 - \hat{\rho}^2}, \quad (76)$$

We obtain

$$0 = \beta^2 + 2\sqrt{m^2 - \rho^2}(\rho^2 - \mu^2), \quad \rho = \hat{\rho}/\ell, \quad (77)$$

which matches the resonance condition found by George [15] for the case of a Minkowski brane in a Minkowski bulk (with an appropriate change of notation $\rho^2 \rightarrow \rho^2 + m^2$ and choice of branch $\sqrt{-\rho^2} = -i\rho$).

4. High energy

The high-energy limit is

$$H\ell \gg 1, \quad \gamma \sim H\ell \gg 1. \quad (78)$$

Unlike the low energy limit above, we make no assumptions about the magnitude of ω . Using the asymptotic expansion for $Q_{i\omega\pm 1/2}^\alpha(\gamma)$ for large γ [23, 8.776(2)], and working to lowest order in $(H\ell)^{-1}$, we find that the resonant condition $\mathcal{R}_\omega = 0$ reduces to:

$$\frac{\beta^2}{H^3} = \frac{1}{i\omega + 1} \left(\omega^2 + \frac{9}{4} - \frac{\mu^2}{H^2} \right) \left(2\omega^2 + i\omega + 3 - \frac{m^2}{H^2} \right),$$

[μ/H and $m\ell$ non-infinite]. (79)

Note that the resonance condition is independent of ℓ , which is expected because the characteristic curvature scale on the brane H^{-1} is much smaller than the characteristic curvature scale of the bulk ℓ ; i.e., the brane “sees” the bulk as flat.

Eq. (79) implies that there are four resonant frequencies that are the solutions of a quartic polynomial. The critical coupling is again obtained by setting $\omega = -3i/2$:

$$\beta_{\text{crit}}^2 = \frac{2}{5} m^2 \mu^2 H^{-1}, \quad (80)$$

which matches the $H\ell \rightarrow \infty$ limit of Eq. (38). As in Sec. III C 2, we can linearise the resonance condition about the zero mode (55), resulting in the perturbation of its Kaluza-Klein mass:

$$\delta\rho_{\text{zero}}^2 \sim \frac{3}{5} m^2 - \frac{3H}{2\mu^2} \beta^2 = \frac{3}{5} m^2 \left(1 - \frac{\beta^2}{\beta_{\text{crit}}^2} \right). \quad (81)$$

This matches the large $H\ell$ limit of (58), as expected.

Note that the high energy limit (78) does not distinguish between H approaching infinity or ℓ approaching infinity. Hence, it is possible to expand (79) in the case of a flat stationary brane; i.e., $H \rightarrow 0$ and $\ell \rightarrow \infty$. This yields

$$\beta^2 = i\rho^{-1}(\rho^2 - \mu^2)(m^2 - 2\rho^2), \quad \rho = \omega H. \quad (82)$$

Note that this result implicitly assumes the $m \rightarrow 0$ limit, since (79) is only valid when $m\ell$ is non-infinite. It is easy to confirm that this matches the flat space resonance condition obtained in the low energy regime (77) when $m \rightarrow 0$.

IV. 4-DIMENSIONAL EFFECTIVE THEORY AND THE BOUND STATE MASS MATRIX

In this section, we show how many of the qualitative and quantitative properties of the model derived from the spectral analysis in Sec. III are encapsulated by an effective 4-dimensional action. Here, ϕ and q refer to the fields in real space, rather than the spatial Fourier transforms.

To derive this action, let us write

$$\phi(\tau, \mathbf{x}, y) = \varphi_1(\tau, \mathbf{x})\xi(y), \quad q(\tau, \mathbf{x}) = \varphi_2(\tau, \mathbf{x}). \quad (83)$$

We substitute these definitions into the full 5-dimensional action (9) and explicitly perform the integrations over y . We obtain the following 4-dimensional effective action:

$$S_{\text{eff}} = -\frac{1}{2} \int_{\partial\mathcal{M}_b} \left[\sum_{i=1}^2 (\partial^\alpha \varphi_i \partial_\alpha \varphi_i + m_i^2 \varphi_i^2) + 2^{(4)}\beta \varphi_1 \varphi_2 \right]. \quad (84)$$

Here, Greek indices are raised and lowered with the brane metric $h_{\alpha\beta}$. We have defined the effective masses and coupling as

$$m_1^2 = 2m^2 \int_{y_b}^\infty dy N^5(y) \xi^2(y) + 2 \int_{y_b}^\infty dy N^3(y) [\xi'(y)]^2,$$

$$m_2^2 = \mu^2, \quad {}^{(4)}\beta = \beta \xi(y_b), \quad (85)$$

where $N(y) = H\ell(\sinh Hy)^{-1}$. In deriving (84), we have assumed

$$\int_{y_b}^\infty dy N^3(y) \xi^2(y) = \frac{1}{2}. \quad (86)$$

This assumption is equivalent to demanding that the original bulk field is normalisable under the Klein-Gordon inner product (36). Hence, our effective action only gives a valid description of the bound state degrees of freedom in the model. The full action (9) is required if we want to include continuum modes (i.e., scattering states) as well.

The 4-dimensional action (84) represents a pair of coupled massive fields confined to the brane. We can seek mass eigenstate solutions (i.e., eigenfunctions of $\nabla^\alpha \nabla_\alpha$) as follows:

$$\nabla^\alpha \nabla_\alpha \varphi_i = \rho^2 \varphi_i \Rightarrow \mathbf{M} \vec{\varphi} = \rho^2 \vec{\varphi}, \quad (87a)$$

$$\mathbf{M} = \begin{pmatrix} m_1^2 & {}^{(4)}\beta \\ {}^{(4)}\beta & m_2^2 \end{pmatrix}, \quad \vec{\varphi} = \begin{pmatrix} \varphi_1 \\ \varphi_2 \end{pmatrix}. \quad (87b)$$

This matrix equation has a non-trivial solution if ρ^2 is one of the eigenvalues of the mass matrix \mathbf{M} , which are

$$\rho_\pm^2 = \frac{m_1^2 + m_2^2}{2} \left(1 \pm \sqrt{1 + \frac{4({}^{(4)}\beta)^2 - m_1^2 m_2^2}{(m_1^2 + m_2^2)^2}} \right). \quad (88)$$

These are the masses of the two normal modes of the system, which should be identified with the Kaluza-Klein masses of bound state resonances in the full 5-dimensional theory.

The fact that we can have at most two mass eigenstates in the 4-dimensional effective theory is consistent with the results of Sec. III B 4, where we saw that there can be at most two bound state resonances in the full 5-dimensional treatment. Furthermore, we note that one of these modes becomes tachyonic (i.e., $\rho_-^2 < 0$) if

$${}^{(4)}\beta^2 > {}^{(4)}\beta_{\text{crit}}^2 = m_1^2 m_2^2. \quad (89)$$

This again matches our expectations: We have one and only one tachyonic mode if the coupling is sufficiently large.

It is important to note that not all mass eigenstates in the effective theory spectrum correspond to bound states of the full 5-dimensional model. Recall that bound states must have Kaluza-Klein mass within the mass gap, so any mass eigenstates with $\rho_{\pm}^2 > 9H/4$ are not true resonances. We have that ρ_+^2 is bounded from below by $\max(m_1^2, m_2^2)$, while ρ_-^2 is bounded from above by $\min(m_1^2, m_2^2)$. Thus, a necessary condition for there to be two bound state solutions in the effective theory is

$$m_1 < 3H/2, \quad m_2 = \mu < 3H/2. \quad (90)$$

Qualitatively, this matches the results of Sec. III B 4, where we saw that a necessary condition for the existence of two bound states was that the field masses were not too heavy. Unfortunately, one cannot translate these inequalities into more stringent constraints on m without knowing $\xi(y)$. We should briefly mention the Minkowski brane case: When $H = 0$ there is no mass gap and only tachyonic resonances with $\rho^2 < 0$ correspond to bound states. Hence, in the effective theory there is only a single tachyonic bound state for supercritical coupling, in agreement with the conclusions of Ref. [16].

We can quantitatively compare our effective theory to the results previously obtained for the perturbed zero mode in Sec. III C 2. We assume that the extra-dimensional profile is the purely “zero mode” solution, as given by Eq. (56):

$$\xi(y) = \text{constant}. \quad (91)$$

Under this assumption, the various integrals in (85) and (86) can be reduced to elementary functions. We find

$$\begin{aligned} \xi^2 &= \ell^{-1} f(H\ell), \quad m_1^2 = m^2 g(H\ell), \\ {}^{(4)}\beta^2 &= \ell^{-1} \beta^2 f(H\ell), \end{aligned} \quad (92)$$

where f and g are defined in Eqs. (59). To relate these back to the perturbed zero mode, recall that our results for $\delta\rho_{\text{zero}}^2$ were derived for the case when m and β were small. This suggests that we expand the effective theory resonant masses (88) under the conditions $m_2^2 \gg \max(m_1^2, {}^{(4)}\beta)$, which yields

$$\rho_+^2 \sim m_2^2 + {}^{(4)}\beta^2/m_2^2, \quad \rho_-^2 \sim m_1^2 - {}^{(4)}\beta^2/m_2^2. \quad (93)$$

Substituting (92) and $m_2 = \mu$ into the above expression for ρ_-^2 , we recover the the 5-dimensional prediction for $\delta\rho_{\text{zero}}^2$ (58). Finally, we note that the effective theory prediction of the critical coupling (89) in this regime is

$${}^{(4)}\beta_{\text{crit}}^2 = \mu^2 m^2 g(H\ell) \sim \ell^{-1} f(H\ell) \beta_{\text{crit}}^2, \quad (94)$$

where we have made use of (60). The relationship between ${}^{(4)}\beta_{\text{crit}}^2$ and β_{crit}^2 is entirely consistent with what we expect from (92).

To summarize this section, we have shown that the bound state sector of our model can be described by the effective action of a pair of coupled scalars propagating on a de Sitter background. The main complication is

that the effective 4-dimensional masses and coupling depend on higher-dimensional details, so moving from the 5-dimensional to 4-dimensional pictures requires the non-trivial calculations performed in the rest of the paper.

V. NUMERIC TIME DOMAIN ANALYSIS

We now turn to the solution of the coupled equations (10) subject to the boundary condition (11) in the time domain. As in Sec. III, we will work with the spatial Fourier transforms (12) of ϕ and q and omit the \mathbf{k} subscript.

A. Dimensionless wave equations in Poincaré coordinates

In our numeric integrations, we elect to use dimensionless versions of the Poincaré coordinates t and z (2), as well as the conformal time η (5). In particular, we define

$$\begin{aligned} \hat{t} &= t/z_*, & \hat{z} &= z/z_*, & \hat{\eta} &= \eta/z_*, \\ \hat{\partial}_t &= \partial/\partial\hat{t}, & \hat{\partial}_z &= \partial/\partial\hat{z}, & \hat{\partial}_\eta &= \partial/\partial\hat{\eta}, \end{aligned} \quad (95)$$

where z_* is a length scale we specify later. We rescale the bulk field as follows

$$\psi(t, z) = \ell^{1/2} \hat{z}^{-3/2} \phi(t, z), \quad (96)$$

and write the brane trajectory as

$$\hat{t}_b = \gamma \hat{\eta}, \quad \hat{z}_b = -H\ell \hat{\eta}, \quad d\hat{\eta}^2 = d\hat{t}_b^2 - d\hat{z}_b^2. \quad (97)$$

Then, the wave equations (10) and boundary condition (11) reduce to

$$0 = [\hat{\partial}_t^2 - \hat{\partial}_z^2 + V(\hat{z})]\psi, \quad (98a)$$

$$0 = [\hat{\partial}_\eta^2 + A(\hat{z}_b)\hat{\partial}_\eta + B(\hat{z}_b)]q + C(\hat{z}_b)\psi_b, \quad (98b)$$

$$0 = (\hat{\partial}_n \psi)_b - D(\hat{z}_b)\psi_b - E(\hat{z}_b)q - F(\hat{z}_b)\hat{\partial}_\eta q, \quad (98c)$$

where the potential is

$$V(\hat{z}) = k^2 z_*^2 + \frac{1}{4}(15 + 4m^2 \ell^2) \hat{z}^{-2}, \quad (98d)$$

the coefficients are

$$\begin{aligned} A(\hat{z}_b) &= 2H\ell \hat{z}_b^{-1}, & D(\hat{z}_b) &= -\frac{3}{2}\gamma \hat{z}_b^{-1}, \\ B(\hat{z}_b) &= k^2 z_*^2 + \mu^2 \ell^2 \hat{z}_b^{-2}, & E(\hat{z}_b) &= \frac{1}{2}\beta \ell^{3/2} \hat{z}_b^{-5/2}, \\ C(\hat{z}_b) &= \beta \ell^{3/2} \hat{z}_b^{-1/2}, & F(\hat{z}_b) &= 0, \end{aligned} \quad (98e)$$

and the (flat-space) normal derivative operator is

$$\hat{\partial}_n = -H\ell \hat{\partial}_t + \gamma \hat{\partial}_z. \quad (98f)$$

Note that even though the F coefficient is zero for the problem at hand, we retain it to keep the algorithm developed in the next section reasonably general.

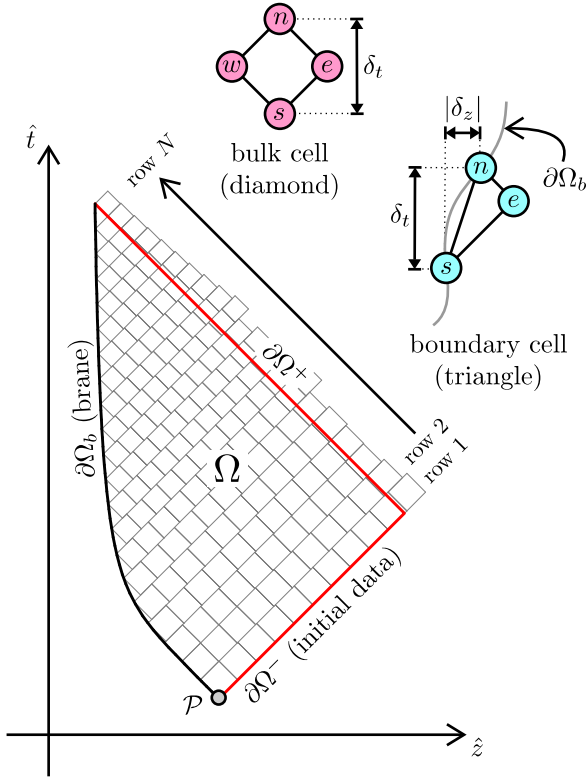


FIG. 6: The spacetime domain Ω over which we seek a numeric solution of (98). Superimposed on Ω is a (particularly coarse) example of the computational grid we use to discretize the problem. Details of the two types of cellular geometries are shown in the upper right corner.

B. The algorithm

Previously, Seahra [18] has developed a numeric algorithm to solve for ψ in equations similar to (98) when there is no brane-bulk coupling ($\beta = 0$) and the brane trajectory is arbitrary. Here, we generalize that procedure to the case when there is a dynamical degree of freedom on the brane.

We seek the numeric solution for ψ throughout a finite region of the (\hat{t}, \hat{z}) plane Ω depicted in Fig. 6, as well as the solution for q on a finite segment $\partial\Omega_b$ of the brane trajectory. To have a well-posed Cauchy evolution for the fields, we must specify initial data for ψ on the past null boundary of the computational domain $\partial\Omega^-$, as well as the value of q and $\hat{\partial}_\eta q$ at $\mathcal{P} = \partial\Omega_b \cap \partial\Omega^-$.

As in Ref. [18], our strategy will be to partition Ω into a large number of small cells to construct a discrete approximation to the fields. In Fig. 6, we see that the cells bounding the brane take the shape of triangles with one timelike and two null sides, while the cells interior to Ω are diamonds with equal null sides. By integrating the bulk wave equation (98a) across a diamond cell, one can find out the value of ψ at the northern node of the cell (i.e., the uppermost corner) in terms of its value at the

other three nodes (cf. [18]):

$$\psi_n = -\psi_s + (\psi_w + \psi_e)(1 - \frac{1}{8}\delta_t^2 V_s) + \mathcal{O}(\delta_t^4), \quad (99)$$

where $\delta_t = \hat{t}_n - \hat{t}_s$ is the difference between \hat{t} evaluated at the top and bottom of the cell. The subscripts n, s, e and w indicate the value of a quantity at the northern, southern, eastern and western nodes, respectively.

The evolution across a triangular cell is more complicated due to the presence of the boundary degree of freedom q . It is useful to re-write the second-order ODE (98b) as a system of two first-order equations

$$\hat{\partial}_\eta q = p, \quad 0 = \hat{\partial}_\eta p + A(\hat{z}_b)p + B(\hat{z}_b)q + C(\hat{z}_b)\psi_b. \quad (100)$$

These can be discretized across a given triangular cell using the modified Euler method:

$$q_n = q_s + \frac{1}{2}\delta_\eta(p_n + p_s) + \mathcal{O}(\delta_\eta^3), \quad (101a)$$

$$p_n = p_s - \frac{1}{2}\delta_\eta(A_n p_n + A_s p_s + B_n q_n + B_s q_s + C_n \psi_n + C_s \psi_s) + \mathcal{O}(\delta_\eta^3). \quad (101b)$$

Also, by integrating (98a) over the cell and making use of (98c) we obtain

$$\begin{aligned} \psi_n = & -\frac{6\delta_\eta(E_n q_n + E_s q_s + F_n p_n + F_s p_s)}{12 + 6\delta_\eta D_n + \delta_u \delta_v V_n} \\ & - \frac{12 + 6\delta_\eta D_s + \delta_u \delta_v V_s}{12 + 6\delta_\eta D_n + \delta_u \delta_v V_n} \psi_s \\ & + \frac{24 - \delta_u \delta_v V_e}{12 + 6\delta_\eta D_n + \delta_u \delta_v V_n} \psi_e + \mathcal{O}(\delta_t^3). \end{aligned} \quad (102)$$

Here,

$$\begin{aligned} \delta_u &= \delta_t - \delta_z, & \delta_v &= \delta_t + \delta_z, & \delta_\eta &= (\delta_t^2 - \delta_z^2)^{1/2}, \\ \delta_t &= \hat{t}_n - \hat{t}_s, & \delta_z &= \hat{z}_n - \hat{z}_s. \end{aligned} \quad (103)$$

By solving the linear system (101) and (102), we can obtain the future field values (q_n, p_n, ψ_n) in terms of the past field values $(q_s, p_s, \psi_s, \psi_e)$.

Having written down these evolution formulae, the actual algorithm for obtaining ψ and q is very similar to the one used in Ref. [18]. Consider the first row of cells in Fig. 6. If we know the value of ψ along $\partial\Omega^-$ as well as the value of (q, p) at \mathcal{P} , then application of the triangle and diamond evolution formulae in sequence (i.e. southwest to northeast) allows us to obtain (q, p, ψ) on the future boundary of the first row. One can then find the values of ψ on the nodes of the past boundary of the second row via interpolation. By repeating this procedure for rows 2 through N , one obtains the solution for the fields throughout Ω . As in Ref. [18], we expect our numeric solutions for ψ and q to converge like δ_t^2 to the actual field values.

C. Results

1. Minkowski brane

We now apply our algorithm to the problem introduced in Sec. II. First, let us consider the simpler case of a brane stationary with respect to the Poincaré frame:

$$H\ell = 0, \quad z_b = \ell, \quad ds_b^2 = -d\tau^2 + d\mathbf{x}^2; \quad (104)$$

i.e., a brane with Minkowski geometry. In this case, we select

$$z_* = \ell \Rightarrow \hat{z}_b = 1. \quad (105)$$

As discussed in Sec. III C 3, the time dependence of any given resonant mode in this case is given by

$$\phi_\omega^R \propto e^{i\varpi t/\ell}, \quad \varpi = \sqrt{\hat{\rho}^2 + k^2\ell^2}, \quad (106)$$

where $\hat{\rho}$ is a solution of the low energy resonance condition (71) with $H\ell = 0$.

As discussed in Sec. III B 1, we expect the late time behaviour of ϕ and q to be dominated by resonant mode solutions at late times, no matter what initial data is selected on $\partial\Omega^-$. Furthermore, if we wait long enough the resonant mode with the smallest imaginary part — which we call the fundamental mode — will dominate the other modes. Hence for any choice of initial data, we expect that

$$q \xrightarrow{t \rightarrow \infty} \text{Re}(C_q e^{i\varpi_0 t/\ell}), \quad \phi_b \xrightarrow{t \rightarrow \infty} \text{Re}(C_\phi e^{i\varpi_0 t/\ell}), \quad (107)$$

where C_q and C_ϕ are complex numbers, and ϖ_0 is the frequency of the fundamental mode.

In Fig. 7, we show the results of our numeric simulations for the following choice of initial data:

$$q(\mathcal{P}) = 1, \quad p(\mathcal{P}) = 0 = \phi(\partial\Omega^-). \quad (108)$$

We find excellent qualitative and quantitative agreement between the simulation results and the expectations for the fundamental frequency from the spectral analysis. In particular, we get exponentially diverging fields (i.e. tachyonic resonances) for large coupling. We further test the agreement between simulations and the resonance condition (71) in Fig. 8.

2. De Sitter brane

For a de Sitter brane, we select z_* to be the position of the brane when the mode under consideration exits the Hubble horizon, which implies

$$kz_* = H\ell. \quad (109)$$

Along the same lines as our discussion of the Minkowski brane above, we expect that the late time behaviour of

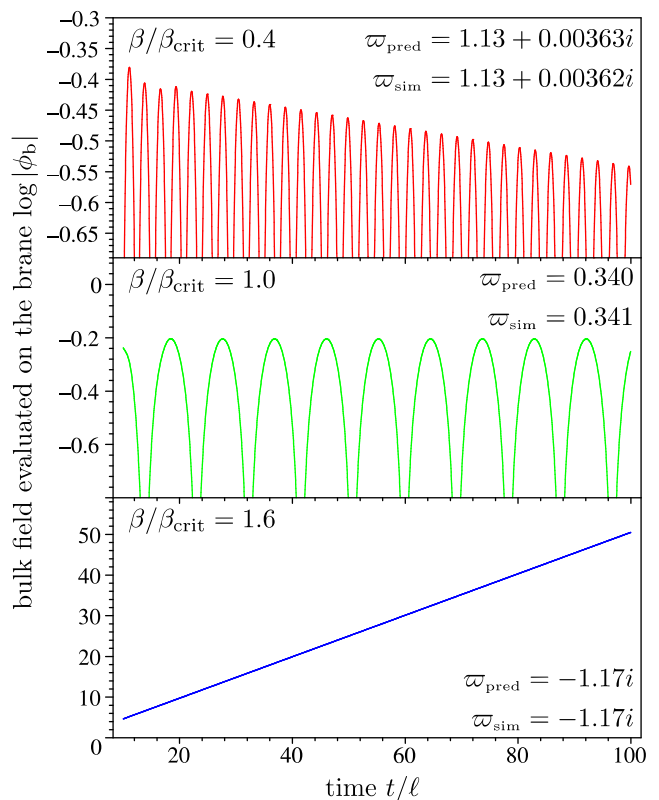


FIG. 7: Simulation results for a Minkowski brane with $\mu\ell = 1.23$, $m\ell = 2.37$ and $k\ell = 0.340$ and the initial data (108). The quoted values of ϖ_{pred} are predictions for the fundamental frequency from the low energy resonance condition (71), while ϖ_{sim} is the late time frequency obtained by fitting the template (107) to the numeric waveforms. This plot exhibits the three possible classes of asymptotic field behavior when $H\ell = 0$.

the fields in a numeric simulation to be

$$q \xrightarrow{\tau \rightarrow \infty} \text{Re} \left[C_q e^{(i\omega_0 - 3/2)H\tau} \right], \quad (110a)$$

$$\phi_b \xrightarrow{\tau \rightarrow \infty} \text{Re} \left[C_\phi e^{(i\omega_0 - 3/2)H\tau} \right], \quad (110b)$$

regardless of the particular choice of initial data. Here, the fundamental frequency ω_0 is the solution of (29) with the smallest imaginary part.

In Fig. 9, we show results for some of our simulations. The particular case considered is one in which the fundamental mode is a scattering state for $\beta/\beta_{\text{crit}} \lesssim 0.65$, and an overdamped bound state for $0.65 \lesssim \beta/\beta_{\text{crit}} < 1$. In Fig. 10, we quantitatively compare the value of the fundamental frequency obtained from the spectral analysis and the value obtained from simulations in a case where there is an overdamped bound state for all subcritical couplings. We find acceptable agreement between the values of ω_0 obtained in both approaches.

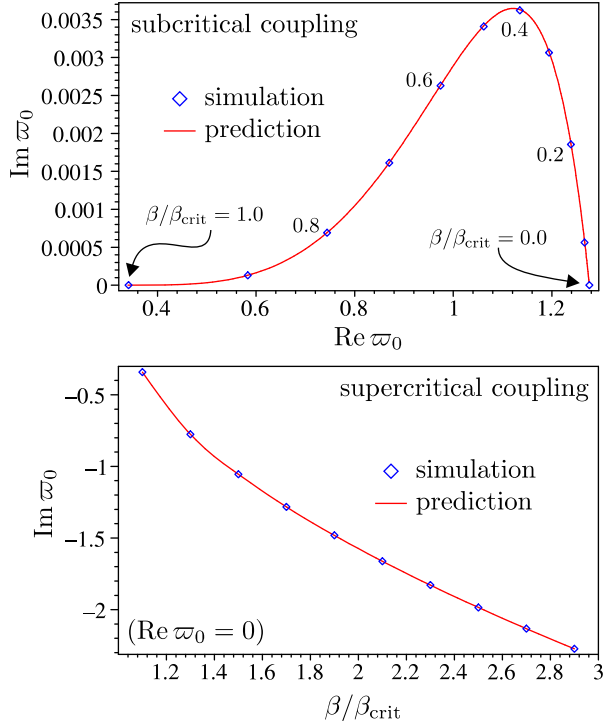


FIG. 8: Comparison between spectral analysis predictions for the fundamental frequency and simulation results when $\mu\ell = 1.23$, $m\ell = 2.37$ and $k\ell = 0.340$ (Minkowski brane).

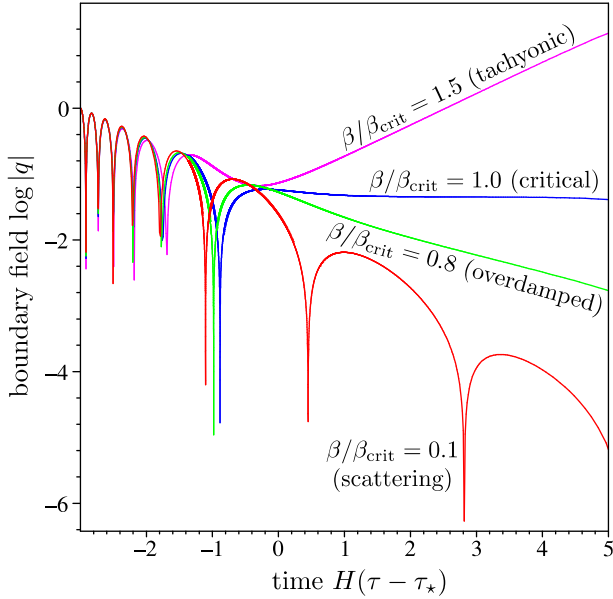


FIG. 9: Simulation results for a de Sitter brane with $\mu\ell = 0.40$, $m\ell = 2.1$ and $H\ell = 0.20$ and the initial data (108). Here, τ_* is the proper time coordinate on the brane when the mode exits the Hubble horizon. Individual curves are labeled by the coupling parameter and the classification of the fundamental mode solution of (29) for these parameters—the four possible varieties of late time behaviour when $H\ell > 0$ are all seen in this plot.

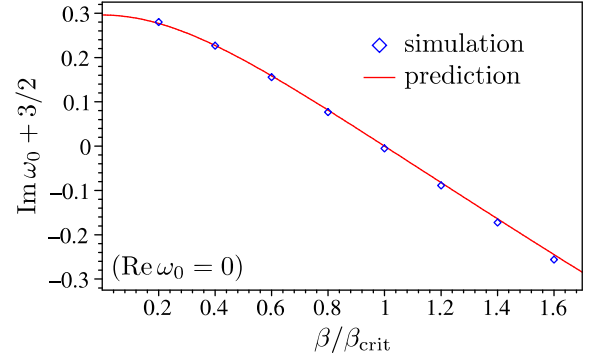


FIG. 10: Comparison between spectral analysis predictions for the fundamental frequency from the full resonance condition $\mathcal{R}_\omega = 0$ and simulation results when $\mu\ell = 1.00$, $m\ell = 2.24$ and $H\ell = 1.12$ (de Sitter brane). For this choice of parameters, the fundamental resonance is never a scattering state.

VI. CONCLUSIONS

In this paper we have studied resonant modes of a massive bulk field in five-dimensional anti-de Sitter spacetime linearly coupled to a massive field on a four-dimensional boundary de Sitter brane. Using spectral scattering theory in 5 dimensions, we investigated the resonant excitations of the system, identifying scattering states which propagate to future null infinity and normalisable bound states. By dimensionally reducing the full action, we have also derived an effective 4-dimensional theory that gives a valid description of the bound state resonances. The effective theory is essentially that of a pair of coupled massive brane-confined scalars.

From the 5-dimensional treatment, we find that the bound state sector of the spectrum is characterised by zero, one, or two resonances. These can be divided into two categories: overdamped and tachyonic modes which decay or diverge exponentially at late times, respectively. We find that there is a critical coupling β_{crit} , above which there always exists a unique tachyonic mode; conversely, no tachyonic bound state exists for subcritical coupling. The critical coupling is given analytically by Eq. (38), and we find that $\beta_{\text{crit}} = 0$ if either field is massless.

All of these bound state properties are mirrored in the effective 4-dimensional theory: namely, the effective action predicts the existence of at most two mass eigenstates, or normal modes, which correspond to bound states of the higher-dimensional theory. Furthermore, one of the normal modes is tachyonic when the coupling exceeds a critical value, and that critical value is zero if either of the effective field masses vanish.

One of the more interesting features of our model is the existence of overdamped bound states, which do not appear in the case of a Minkowski brane in an AdS bulk [16]. It is well known that for a Minkowski brane, all bulk modes with real Kaluza-Klein mass reduce to travelling

waves far from the brane and are hence non-normalisable. However for a de Sitter brane, it is possible to have normalisable bulk modes with Kaluza-Klein mass less than $3H/2$ [17]. The overdamped bound states found in this paper live within this mass gap, which explains why they are not present when the brane is “at rest” ($H = 0$). For these stationary branes, one can only have a single tachyonic bound state, and that state only exists for supercritical coupling.

The actual number of bound states for a given choice of parameters is strongly influenced by the masses of the bulk and brane fields. In particular, a necessary condition for the existence of two bound state resonances is that both fields are “light” compared to the Hubble scale. In this context, the notions of light and heavy refer to the behaviour of the individual fields at zero coupling. The brane scalar is considered to be light if it does not oscillate on super-horizon scales when $\beta = 0$. Quantitatively, this means that the boundary mass is less than $3H/2$. On the other hand, a light bulk scalar is one for which there exists a normalisable bound state in the absence of any brane-localised couplings. We have numerically determined that this is equivalent to demanding that the bulk mass squared m^2 is less than $\sim 4.50 H$ at low energy ($H\ell \ll 1$) and less than $\sim 4.42 H$ at high energy ($H\ell \gg 1$). We can qualitatively recover these necessary conditions for multiple bound states from the effective theory, but we can only obtain the precise bound on m quoted here from the full spectral formalism.

We studied the behaviour of the model’s resonances in a number of different limits in Sec. III C, and have recovered several results previously available in the literature. One case worth emphasizing involves the perturbation of the massless de Sitter zero mode when β and m take on small values. Under these conditions, we have demonstrated that there is complete agreement between the predictions of the 5-dimensional spectral formalism and the 4-dimensional effective theory for the perturbative zero mode mass, critical coupling, etc. In particular, we find that the perturbed zero mode mass is given by $\delta\rho_{\text{zero}}^2 \sim \frac{1}{2}m^2(1 - \beta^2/\beta_{\text{crit}}^2)$ for $H\ell \ll 1$ and $\delta\rho_{\text{zero}}^2 \sim \frac{3}{5}m^2(1 - \beta^2/\beta_{\text{crit}}^2)$ for $H\ell \gg 1$. From the condition that the the Kaluza-Klein masses of normalisable states must lie within the mass gap, we have confirmed that a necessary condition for a bulk bound state at zero coupling is $m^2/H^2 < 9/2$ for $H\ell \ll 1$, in agreement with

the numerical results of Sec. III C 1.

We have tested the predictions of the spectral theory against a new numerical algorithm that is able to evolve the coupled brane and bulk fields. We are able to confirm our spectral analysis predictions for the fundamental frequencies by studying the late-time behaviour for both a static (Minkowski) brane and a moving de Sitter brane in the Poincaré coordinates. In particular we find good quantitative agreement between the rate of decay or growth of the boundary field and the imaginary part of the frequency of the fundamental mode for both subcritical and supercritical coupling.

We have chosen to work with a moving brane Poincaré coordinates so that the code can also be used to study cosmological branes with arbitrary trajectories in AdS. Our numerical code can be used to study the coupled evolution any system where the bulk and boundary wave equations and boundary condition can be written in form given in Eqs. (98). We will thus be able to study coupled bulk and brane fields in situations where we have no analytic results to compare against. For instance such a numerical code is required to study the evolution of cosmological density perturbations consistently coupled to bulk metric perturbations during the matter- or radiation-dominated eras.

The simple model of linearly coupled bulk and brane fields on a de Sitter brane which we have considered in this paper may be a useful toy model for the study of inflaton perturbations linearly coupled to scalar metric perturbations during inflation in a higher-dimensional bulk. However the inflaton-metric interaction involves derivative couplings which makes the problem considerably more challenging. In particular we find that the bulk field is coupled to an infinite tower of bulk modes [12, 13, 30]. We will return to this problem in future work.

Acknowledgments

AC is supported by FCT (Portugal) PhD fellowship SFRH/BD/19853/2004. KK and SSS are supported by PPARC. AM is supported by PPARC grant PPA/G/S/2002/00576.

-
- [1] L. Randall and R. Sundrum, Phys. Rev. Lett. **83**, 4690 (1999), hep-th/9906064.
 - [2] S. Mukohyama, Phys. Rev. **D62**, 084015 (2000), hep-th/0004067.
 - [3] H. Kodama, A. Ishibashi, and O. Seto, Phys. Rev. **D62**, 064022 (2000), hep-th/0004160.
 - [4] C. van de Bruck, M. Dorca, R. H. Brandenberger, and A. Lukas, Phys. Rev. **D62**, 123515 (2000), hep-th/0005032.
 - [5] K. Koyama and J. Soda, Phys. Rev. **D62**, 123502 (2000), hep-th/0005239.
 - [6] S. Mukohyama, Class. Quant. Grav. **17**, 4777 (2000), hep-th/0006146.
 - [7] D. Langlois, Phys. Rev. Lett. **86**, 2212 (2001), hep-th/0010063.
 - [8] H. A. Bridgman, K. A. Malik, and D. Wands, Phys. Rev. **D65**, 043502 (2002), astro-ph/0107245.
 - [9] S. S. Seahra, Phys. Rev. **D72**, 066002 (2005), hep-

- th/0501175.
- [10] S. S. Seahra, C. Clarkson, and R. Maartens, *Class. Quant. Grav.* **22**, L91 (2005), gr-qc/0504023.
- [11] C. Clarkson and S. S. Seahra, *Class. Quant. Grav.* **22**, 3653 (2005), gr-qc/0505145.
- [12] K. Koyama, D. Langlois, R. Maartens, and D. Wands, *JCAP* **0411**, 002 (2004), hep-th/0408222.
- [13] K. Koyama, S. Mizuno, and D. Wands, *JCAP* **0508**, 009 (2005), hep-th/0506102.
- [14] T. Hiramatsu and K. Koyama (2006), hep-th/0607068.
- [15] A. George, *J. Phys.* **A38**, 7399 (2005), hep-th/0412067.
- [16] K. Koyama, A. Mennim, and D. Wands, *Phys. Rev.* **D72**, 064001 (2005), hep-th/0504201.
- [17] J. Garriga and M. Sasaki, *Phys. Rev.* **D62**, 043523 (2000), hep-th/9912118.
- [18] S. S. Seahra, *Phys. Rev.* **D74**, 044010 (2006), hep-th/0602194.
- [19] T. Hiramatsu, K. Koyama, and A. Taruya, *Phys. Lett.* **B578**, 269 (2004), hep-th/0308072.
- [20] K. Ichiki and K. Nakamura, *Phys. Rev.* **D70**, 064017 (2004), hep-th/0310282.
- [21] K. Ichiki and K. Nakamura (2004), astro-ph/0406606.
- [22] T. Hiramatsu, K. Koyama, and A. Taruya, *Phys. Lett.* **B609**, 133 (2005), hep-th/0410247.
- [23] I. S. Gradshteyn and I. M. Ryzhik, *Table of Integrals, Series, and Products* (Academic Press, London, 1980), 5th ed.
- [24] J. R. Taylor, *Scattering Theory* (Wiley, New York, 1972).
- [25] L. D. Landau and E. M. Lifshitz, *Quantum Mechanics (Non-relativistic theory)*, vol. 3 of *Course of Theoretical Physics* (Elsevier, London, 1977), 3rd ed.
- [26] H.-P. Nollert, *Class. Quantum Grav.* **16**, R159 (1999).
- [27] N. Sago, Y. Himemoto, and M. Sasaki, *Phys. Rev.* **D65**, 024014 (2002), gr-qc/0104033.
- [28] Y. Himemoto and M. Sasaki, *Phys. Rev.* **D63**, 044015 (2001), gr-qc/0010035.
- [29] D. Langlois and M. Sasaki, *Phys. Rev.* **D68**, 064012 (2003), hep-th/0302069.
- [30] K. Koyama, A. Mennim, V. A. Rubakov, D. Wands, and T. Hiramatsu (2007), hep-th/0701241.